

Non-isothermal Crystallization Kinetics and Melting Behaviors of Poly(butylene succinate) and Its Copolyester Modified with Trimellitic Imide Units

Xiaoqing Liu,^{1,2} Chuncheng Li,¹ Yaonan Xiao,¹ Dong Zhang,¹ Wan Zeng³

¹Key Laboratory of Engineering Plastics, Joint Laboratory of Polymer Science and Materials, Center for Molecular Science, Institute of Chemistry, Chinese Academy of Sciences, Beijing 100080, People's Republic of China

²Graduate School of the Chinese Academy of Sciences, Beijing 100039, People's Republic of China

³Department of Chemistry, Xiang Tan University, Xiang Tan, People's Republic of China

Received 12 December 2005; accepted 11 April 2006

DOI 10.1002/app.24625

Published online in Wiley InterScience (www.interscience.wiley.com).

ABSTRACT: With the help of differential scanning calorimeter (DSC), the basic thermal behaviors, nonisothermal crystallization kinetics, and subsequent melting behaviors of poly(butylene succinate) (PBS) and its copolyester (PBSTMA) modified with trimellitic imide units were investigated in this paper. The DSC thermograms of PBS and PBSTMA showed that the crystallization behaviors of PBS were affected seriously because of the addition of a small quantity of trimellitic imide units. The nonisothermal crystallization processes of them were represented by the Avrami equation modified by Jeziorny and the method

developed by Ozawa. After that, the conception of "crystallization rate coefficient (CRC)" introduced by Khanna was employed. The values of CRC for PBS and PBSTMA are 174.6 and 88.2 h⁻¹, respectively. At the end of this paper, the melting behaviors of PBS and PBSTMA after being cooled from 130 to 30°C at different cooling rate were studied in detail. © 2006 Wiley Periodicals, Inc. *J Appl Polym Sci* 102: 2493–2499, 2006

Key words: poly(butylene succinate); trimellitic imide units; nonisothermal crystallization kinetics; melting behaviors

INTRODUCTION

With the development of society and improvement of human life, the utility of biodegradable polymers has received much more attention¹ due to the potential applications in the recent years. Aliphatic polyesters are one of the most promising structural materials for biodegradable or compostable fibers, non-wovens, films, sheets, bottles, and injection-molded products.² However, its full-scale commercialization met with obstruction because of its poorer mechanical properties and higher cost compared with other universal plastics.^{3,4}

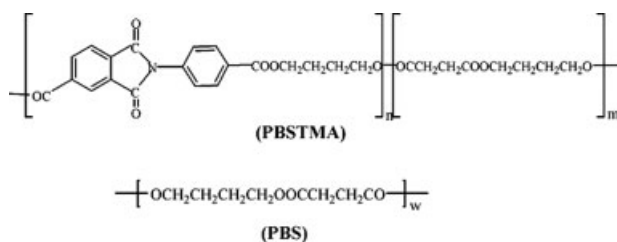
Poly(butylene succinate) (PBS) is one of the best members in the family of aliphatic polyesters because of its relatively high melting point. So far, to promote its physical properties or extend its application fields, a number of techniques, such as physical blending and copolymerization, have been used. At the same time, many new copolymers of PBS have been reported in several literatures.^{5–8} However, in the case of PBS, these modifications have been little

investigated compared with other aliphatic polyesters. In particular, the studies on crystallization behaviors and morphologies were mainly focused on PBS homopolymer^{9–13} and there was in general a lack of this information for PBS copolymer.^{14–17} For example, Wang et al.¹⁴ studied the multiple melting behavior of poly(butylenes succinate-co-adipate) isothermally crystallized from the melt. The crystal structure and growth kinetics of isothermal melt-crystallized poly(butylenes succinate-co-14 mol % ethylene succinate) copolyester have been investigated by Gan et al.¹⁷ In our previous paper,¹⁵ the crystallization behavior and morphology of Poly(butylene succinate) modified with rosin maleopimaric acid anhydride have been reported. It was obvious that these researches on the crystallization process were limited to isothermal condition. However, the crystallization in a varying condition is of practical interest because industrial processes generally proceed under nonisothermal environment. To obtain materials with better physical properties and get the optimum condition in an industrial process, it is necessary to compare the nonisothermal crystallization properties of different polymer systems.

Polyimides are one of the most important commercial polymers because of their good thermal properties and mechanical properties. To our knowledge, the combination of polyesters and polyimides

Correspondence to: C.-C. Li (lizy@iccas.ac.cn).

Contract grant sponsor: National Natural Science Foundation of China; contract grant number: NSFC-50303020.



Scheme 1 The chemical structures for PBSTMA and PBS.

has achieved great success and yielded a series of new materials with high performance.^{18–20} In our previous work,²¹ we introduced rigid trimellitic imide units (TMA) into the main chain of PBS for the first time and found that the mechanical properties of PBS were improved obviously without a notable deterioration of melting temperature. In this paper, the basic thermal properties of the new copolyester (PBSTMA) were investigated. And then several equations for nonisothermal crystallization kinetics were employed to study the nonisothermal crystallization characteristics of PBS and PBSTMA. After that, the melting behaviors of them nonisothermally melt-crystallized were studied in detail.

EXPERIMENTAL

Materials

PBSTMA (denoting the copolyester of PBS modified with trimellitic imide units in this paper) and PBS were synthesized by us as reported in one of our previous papers.²¹ Before characterization and investigation all the polyesters were purified by reprecipitation from chloroform solution using methanol repeatedly followed by drying under vacuum. The composition of the copolyester was determined by ¹H-NMR techniques and the mole percentage of trimellitic imide units in segment was 5.1%. The intrinsic viscosity of PBS and PBSTMA was 1.10 and 0.96 dL/g, respectively, which was determined by viscosimetry in metacresol at (25 ± 0.1)°C at a concentration of 1 g/dL. The chemical structures for PBSTMA and PBS are shown as follows (Scheme 1).

Differential scanning calorimetry

The thermal parameters, nonisothermal crystallization kinetics and melting behaviors studies were carried out using a Perkin–Elmer differential scanning calorimetry (DSC)-7. The calibration of the temperature was performed using indium as the standard before the measurements. All the measurements were conducted under high-purity helium gas.

For basic thermal properties studies, the sample was heated to 150°C quickly, stayed there for 5 min to erase any thermal history, and then quenched to –100°C at

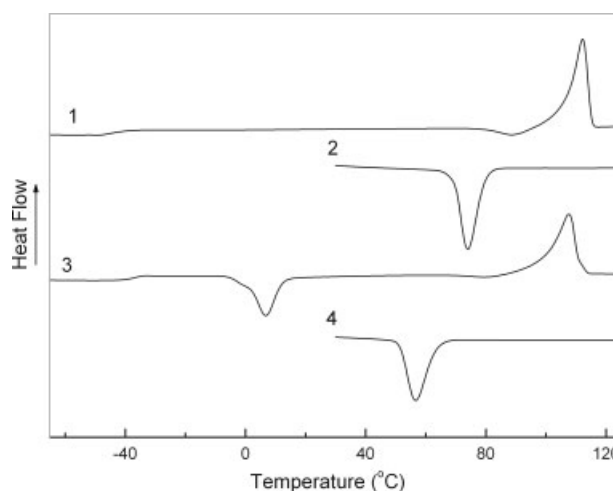


Figure 1 DSC thermograms of PBS and PBSTMA: 1 for PBS heating curve; 3 for PBSTMA heating curve; 2 for PBS cooling curve; 4 for PBSTMA cooling curve.

a rate of 200°C/min. After that, it was heated from –100 to 130°C at a rate of 20°C/min for heating scan and stayed there for 5 min before being cooled to 30°C at the same rate for cooling scan. The endothermic and exothermic curves were recorded to determine the thermal parameters.

The nonisothermal crystallization kinetics and melting behaviors studies were performed as follows: the samples were heated to 150°C and held there for 5 min to eliminated thermal history before cooling the melt to 30°C at different cooling rates. After that, they were reheated from 30 to 130°C at a rate of 20°C/min at once. The cooling and heating curves were recorded. The cooling rates were 5, 10, 15, 20, and 30°C/min respectively.

RESULTS AND DISCUSSION

Basic thermal parameters of PBS and PBSTMA

The basic thermal properties of PBS and PBSTMA were characterized with DSC. Figure 1 showed the

TABLE I
Basic Thermal Parameters of PBS and PBSTMA
Determined by DSC

Sample	T_g^a (°C)	T_{cc}^b (°C)	T_c (°C)	T_m (°C)	ΔT^c (°C)	ΔH_m^d (J/g)
PBS	–43.1	–	73.9	111.7	37.8	65.7
PBSTMA	–38.3	6.8	57.7	106.3	48.6	57.7

^a Glass-transition temperature.

^b Cold crystallization temperature taken from the DSC heating curves.

^c Degree of supercooling. $\Delta T = T_m - T_c$.

^d Enthalpy of fusion.

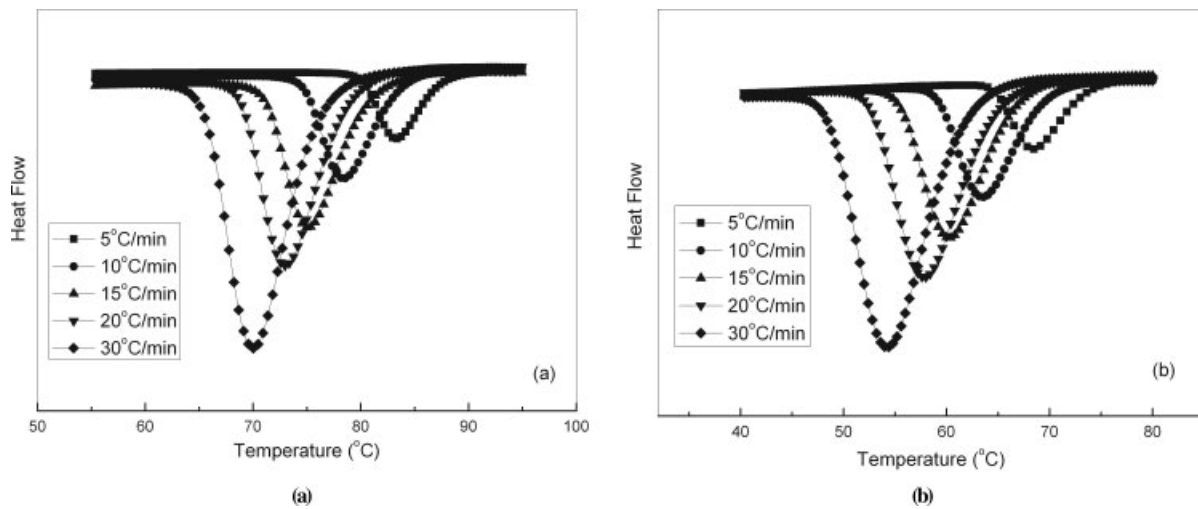


Figure 2 The DSC curves of PBS (a) and PBSTMA (b) cooled from the melt at various cooling rates.

heating curves and cooling curves of them and the interrelated thermal parameters were given in Table I.

From Figure 1 we could see that the heating curve of PBS showed melting temperature (T_m) at 111.7°C, which was little higher than that of PBSTMA (106.3°C). This was in agreement with the general rule of copolymers. But the crystallization temperature (T_c) of PBS was much higher compared with that of PBSTMA. The degree of supercooling ($\Delta T = T_m - T_c$) is an important parameter for determining the crystallization of polymer.²² Generally speaking, an increasing in ΔT means the crystallizability became poorer. In this case, as shown in Table I, the ΔT value of PBS was increased largely when the trimellitic imide units was added. These results showed that the crystallization rate of PBSTMA was much lower than that of PBS. The most important thing we should pay attention to was that the heating curve of PBSTMA showed an obvious cold-crystallization peak at 6.8°C. However, for PBS, the cold-crystallization peak could not be seen. This also meant PBSTMA was more difficult to crystallize compared with PBS in the same condition. Based on these points, in the next section the

crystallization behaviors under nonisothermal conditions of PBS and PBSTMA were discussed in detail.

Nonisothermal crystallization kinetics: Avrami equation modified by Jeziorny

The nonisothermal crystallization exothermic curves of PBS and PBSTMA at various cooling rates (R) are illustrated in Figure 2. T_p is the peak temperature at which the crystallization rate is maximal, and T_p shifts to a lower temperature region with increasing R both for PBS and PBSTMA because of the fact that the motion of the polymer chains can not follow the cooling temperature in time due to the influence of heat hysteresis. This observation is a common phenomenon for semicrystalline polymer being crystallized nonisothermally. It was also seen that, for a given R , the T_p of PBSTMA was lower than that of PBS, which indicated PBS had a higher crystallization rate again.

Based on DSC data, the value of the relative degree of crystallinity $X(t)$ at different crystallization temperature was calculated and Figure 3 presents $X(t)$ as a function of temperature.

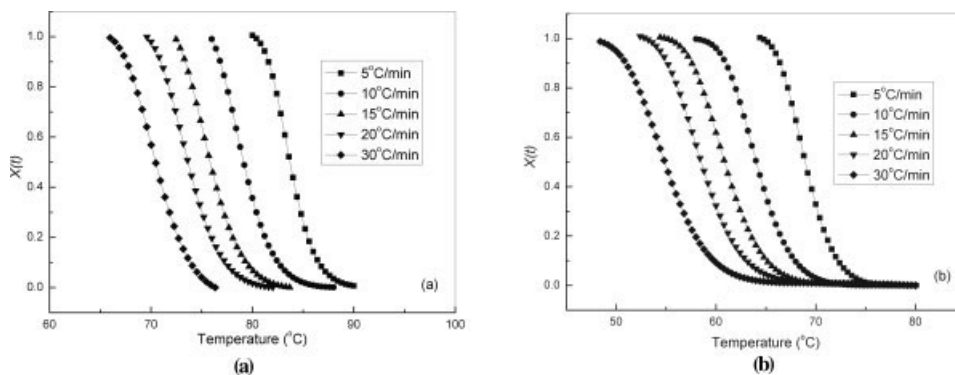


Figure 3 Plots of $X(t)$ as a function of crystallization temperature T (a) for PBS; (b) for PBSTMA.

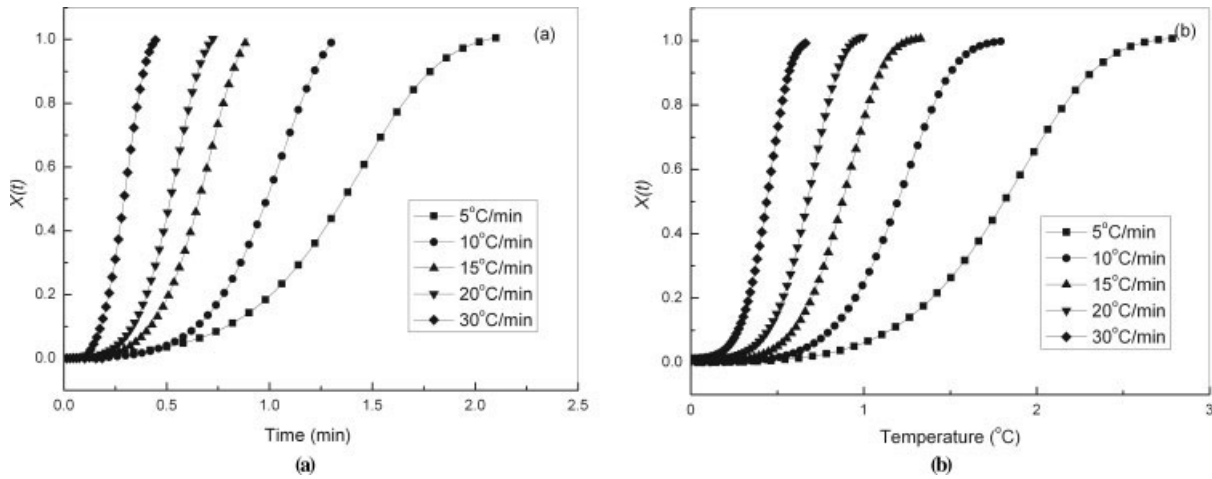


Figure 4 The relative crystallinity as a function of time (a) for PBS; (b) for PBSTMA.

At the same time, the temperature abscissa in Figure 3 could be transformed into a time scale, as shown in Figure 4, based on the following equation:

$$t = (T - T_0)/R \tag{1}$$

where R was the cooling rate, T was the temperature at crystallization time t and T_0 was the onset temperature of crystallization. It could be seen from Figure 4, the higher the cooling rate, the shorter the time of crystallization completion. Because of the spherulite impingement in the later stage, the curves tended to flat and became S-shape, which was in consistent with other polymers reported.

Although the Avrami equation^{23,24} was often used to study the isothermal crystallization behavior of polymers, Mandelkern²⁵ considered that the primary stage of nonisothermal crystallization could be described by the Avrami equation:

$$X(t) = 1 - \exp(-Z_t t^n) \tag{2}$$

$$\ln\{-\ln[1 - X(t)]\} - n \ln t + \ln Z_t \tag{3}$$

where $X(t)$ is the relative degree of crystallinity at time t , Z_t is the rate constant in the nonisothermal crystallization process. Considering the nonisothermal character of the process investigated, Jeziorny suggested that the value of the rate parameter Z_t should be corrected.²⁶ Because the temperature was constantly changing during the process, the final form of the Z_t characterizing the kinetics of nonisothermal crystallization was given as follows:

$$\ln Z_c = \ln Z_t/R \tag{4}$$

By using eq. (3), a plot of $\ln\{-\ln[1 - X(t)]\}$ versus $\ln t$ is shown in Figure 5. The values of Avrami exponent n and the rate parameter Z_t or Z_c determined from the slope and intercept are shown in Table II. The

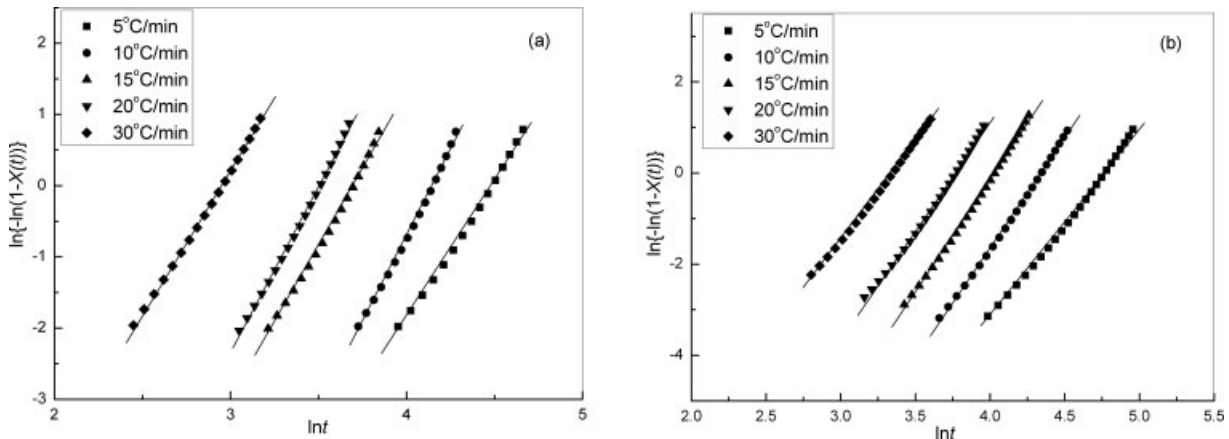


Figure 5 Plots of $\ln\{-\ln[1 - X(t)]\}$ versus $\ln t$ for crystallization of (a) PBS; (b) PBSTMA.

TABLE II
Non-Isothermal Crystallization Kinetics Parameters
of PBS and PBSTMA Based on Avrami Equation
Modified by Jeziorny

R ($^{\circ}\text{C}/\text{min}$)	PBS		PBSTMA	
	Z_c	n	Z_c	n
5	0.032	3.8	0.023	4.1
10	0.184	3.9	0.131	4.7
15	0.357	4.1	0.276	4.6
20	0.458	4.4	0.419	4.8
30	0.677	3.9	0.623	4.3

values of Avrami exponent n for PBSTMA ranged from 4.1 to 4.8 and that of PBS ranged from 3.8 to 4.4 depending on the cooling rate. Apparently, the spherulite growth of them occurred with homogeneous nucleation.²⁷ At the same time, the values of Avrami exponent n for PBSTMA were larger than that of PBS, which meant that the mode of spherulitic growth for PBSTMA might be more complicated than that of PBS. On the other hand, the values of Z_c increased with increasing the cooling rate for both PBS and PBSTMA. At the same cooling rate, the Z_c for PBSTMA was smaller than that of PBS, indicating again the crystallization rate of PBS was higher than that of PBSTMA.

Ozawa models analysis in nonisothermal crystallization

Considering the effect of cooling rate on the nonisothermal crystallization, Ozawa²⁸ shifted the Avrami equation into the case of nonisothermal crystallization by assuming that the sample was cooled with a constant rate from the molten state. According to Ozawa, the relationship between $X(t)$ and R is as follow:

$$\ln\{-\ln[1-X(t)]\} = \ln Kt - n_0 \ln R \quad (5)$$

where $X(t)$ is the relative degree of crystallinity, n_0 is the Ozawa exponent, K_t is the kinetic crystallization rate constant and R is the cooling rate. If the Ozawa

equation could describe the nonisothermal crystallization process very well, drawing the plots of $\ln\{-\ln[1-X(t)]\}$ as a function of $\ln R$, we should get a series of straight lines. Ozawa equation is found to be able to describe the nonisothermal crystallization of many polymers such as poly(trimethylene terephthalate) well.²⁹ It was obvious that, the Ozawa equation failed to describe the nonisothermal crystallization process of PBS [Fig. 6(a)]. On the other hand, Figure 6(b) showed a series of straight lines, from which it was found that Ozawa method could describe the nonisothermal crystallization process successfully. The possible reason might be that the secondary crystallization of PBS was more apparent than that of PBSTMA, which was similar to other report.^{13,30} However, Ozawa took no account of the secondary crystallization and assumed that the Ozawa exponent was constant over the entire crystallization process.²⁸ Therefore, it failed to describe the nonisothermal crystallization process of PBS because of its serious secondary crystallization.

Crystallization rate coefficient

To get a direct comparison of the crystallization rate in the nonisothermal crystallization process on a single scale, Khanna³¹ introduced the "crystallization rate coefficient (CRC)," which represented a change in cooling rate required to bring about 1°C change in the supercooling of the polymer melt.³² The value of CRC could be determined from the slope of the plot of cooling rate versus the crystallization peak temperature T_p . According to the definition, the CRC values are higher for faster crystallization systems.

Figure 7 showed the plots of cooling rate R versus T_p based on Khanna's treatment. The values of CRC obtained from Figure 7 for PBS and PBSTMA were 174.6 and 88.2 h^{-1} , respectively, which was another proof for the higher crystallization rate of PBS compared with that of PBSTMA.

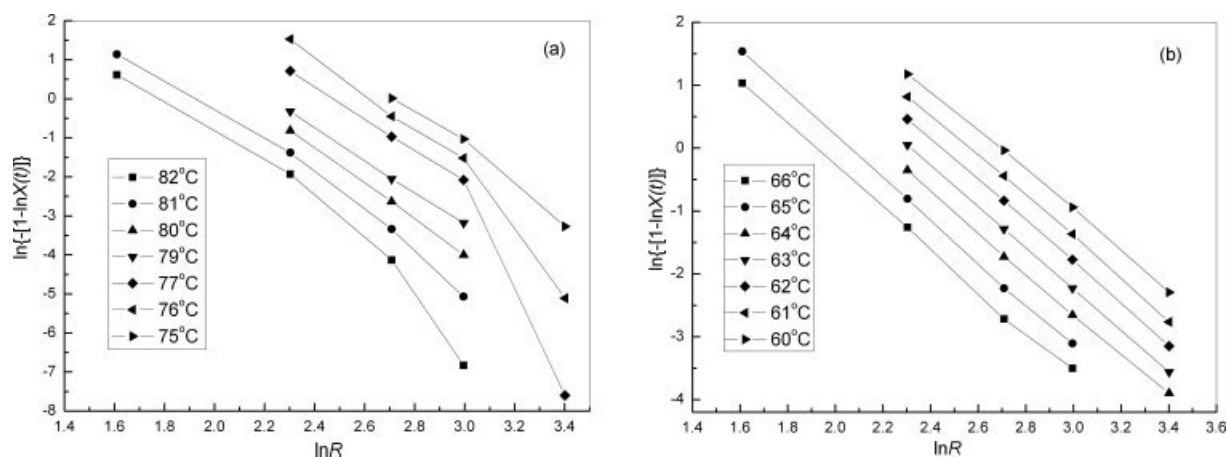


Figure 6 Ozawa plots of PBS and PBSTMA during the nonisothermal crystallization from the melt: (a) PBS; (b) PBSTMA.

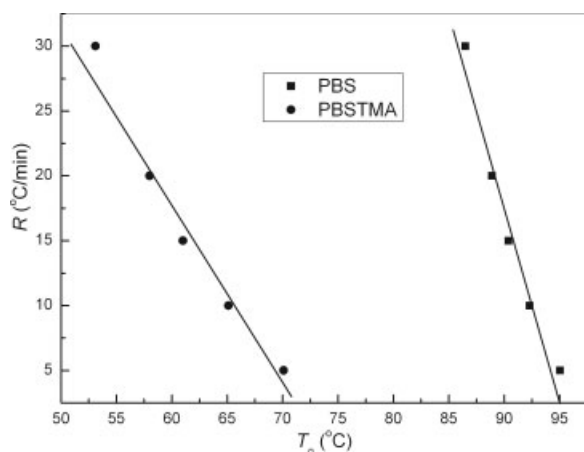


Figure 7 The plots of cooling rate R versus T_p based on Khanna's treatment.

Melting behaviors of PBS and PBSTMA after the nonisothermal crystallization

Figure 8 shows the subsequent melting behaviors of PBS (a) and PBSTMA (b) crystallized from the melt at different cooling rate. It was obvious that the double melting behavior (Peak L and Peak H in Fig. 8) was observed for PBS samples when the cooling rates were lower than $10^\circ\text{C}/\text{min}$. While when the cooling rates were higher ($\geq 15^\circ\text{C}/\text{min}$), it exhibited the single peaks accompanied with a shoulder peak (see the arrow in Fig. 8). But for PBSTMA the appearance of the Peak L was seen only when the cooling rate was lower than $5^\circ\text{C}/\text{min}$. Yasuniwa and Satou³³ and Qiu et al.³⁴ also found that PBS showed double melting peaks after crystallizing nonisothermally from the melt at a constant cooling rate, which was ascribed to the re-crystallization and melting mechanism. That was to say, the low-temperature and high-temperature peaks in the Figure 8 were

attributed to the melting of some amount of the primary crystallites and the melting of the more stable crystals formed through the melt-recrystallization process during the heating scan, respectively. These facts led to the conclusion that there was less re-crystallization growth in PBSTMA compared with that of PBS at the same condition. When the cooling rates were fast enough ($>20^\circ\text{C}/\text{min}$), a broad exothermic peak could be found before the Peak H. At the same time, the temperature of the exothermic peak decreased with increasing cooling rate. Based on these facts, it could be postulated that the melting and recrystallization were competitive in the heating process. The primary crystallites formed during nonisothermal melt-crystallization were not stable enough and, upon subsequent heating, the rate of recrystallization exceeded that of the melting. This fact was true for many other polymers.^{29,33–35}

CONCLUSIONS

The basic thermal properties of PBS and PBSTMA were studied using DSC. The DSC thermograms of PBS and PBSTMA indicated that the crystallizability was affected largely when the trimellitic imide units were added into the chain of PBS. The nonisothermal crystallization processes of PBS and PBSTMA were described by the Avrami equation modified by Jeziorny and the method developed by Ozawa. The crystallization rate of PBSTMA was much slower and the mode of spherulitic nucleation might be more complicated than that of PBS because of the addition of trimellitic imide units. The Ozawa equation could describe the nonisothermal crystallization process of PBSTMA successfully. But for PBS, it did not provide an adequate description because of the serious secondary crystallization. The CRC values determined from the Khanna's treatment were

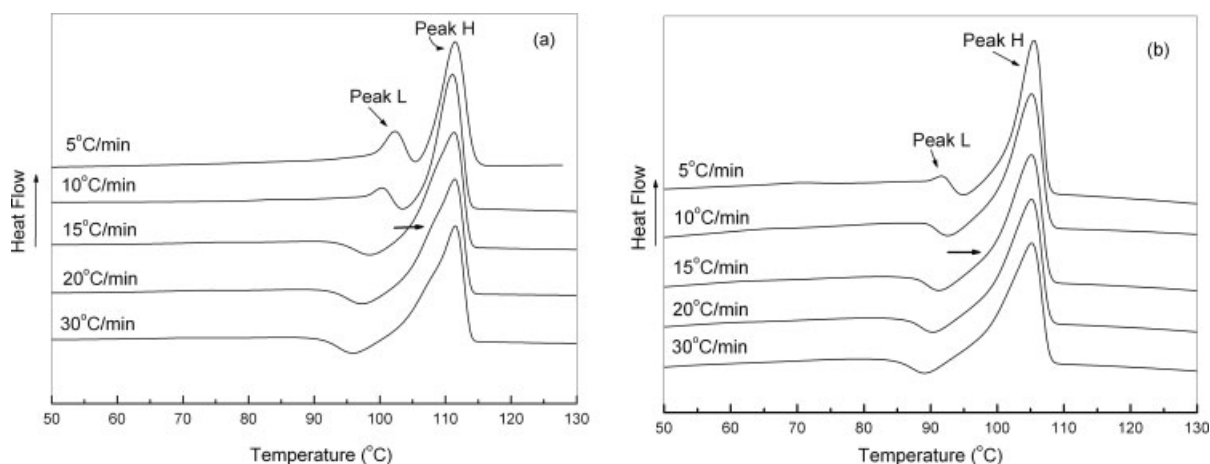


Figure 8 Subsequent melting endotherms for (a) PBS and (b) PBSTMA after nonisothermal crystallization at different rates. The heating rate was $20^\circ\text{C}/\text{min}$.

174.6 and 88.2 h⁻¹ for PBS and PBSTMA, respectively, from which the same outcomes as that in the crystallization kinetics were obtained. The subsequent melting behaviors of PBS and PBSTMA nonisothermal crystallized from the melt were investigated using DSC. The facts led to the conclusion there was less re-crystallization growth in PBSTMA compared with that of PBS at the same condition.

References

1. Lenz, R. W. *Adv Polym Sci* 1993, 1, 107.
2. Fujimaki, T. *Polym Degrad Stab* 1998, 59, 209.
3. Kasuya, K.; Takagi, K.; Ishiwatari, S.; Yoshida, Y.; Doi, Y. *Polym Degrad Stab* 1998, 59, 327.
4. Nagata, M.; Kiyotsukuri, T.; Minami, S.; Tsutsumi, N.; Sakai, W. *Polym Int* 1996, 39, 83.
5. Jin, H. J.; Lee, B. Y.; Kim, M.-N. *J Polym Sci Part B: Polym Phys* 2000, 38, 1504.
6. Jung, I. K.; Lee, K. H.; Chin, I.-J.; Yoon, J. S.; Kim, M. N. *J Appl Polym Sci* 1999, 72, 553.
7. Park, Y. H.; Cho, C. G. *J Appl Polym Sci* 2001, 79, 2067.
8. Cao, A. M.; Takashi, O.; Chieko, I.; Kazwo, N.; Yoshio, I.; Takashi, M. *Polymer* 2002, 43, 671.
9. Ihn, K. J.; Yoo, E. S.; Im, S. S. *Macromolecules* 1995, 28, 2460.
10. Chatani, Y.; Hasegawa, R.; Tadokoro, H. *Polym Prepr Jpn* 1971, 20, 420.
11. Yoo, E. S.; Im, S. S. *J Polym Sci Part B: Polym Phys* 1999, 37, 1357.
12. Miyata, T.; Masuko, T. *Polymer* 1998, 39, 1399.
13. Qiu, Z. B.; Fujinami, S.; Komura, M.; Nakajima, K.; Ikehara, T.; Nishi, T. *Polym J* 2004, 36, 642.
14. Wang, Y. M.; Mrinal, B.; Joao, F. M. *J Polym Sci Part B: Polym Phys* 2005, 43, 3077.
15. Liu, X. Q.; Li, C. C.; Guan, G. H.; Yuan, X. P.; Xiao, Y. N.; Zhang, D. *J Polym Sci Part B: Polym Phys* 2005, 43, 2694.
16. Jun, W. P.; Dong, K. K.; Seung, S. I. *Polym Int* 2002, 51, 239.
17. Gan, Z. H.; Abe, H.; Doi, Y. *Biomacromolecules* 2001, 2, 313.
18. Lips, P. A. M.; Broos, R.; Heeringen, M. J. M.; Dijkstra, P. J.; Feijen, J. *Polymer* 2005, 46, 7827.
19. Qian, Z. Y.; Li, S.; He, Y.; Li, C.; Liu, X. *Polym Degrad Stab* 2003, 81, 279.
20. Pivsa, A. S.; Nakayama, A.; Kawasaki, N.; Yamamoto, N.; Aiba, S. *J Appl Polym Sci* 2002, 85, 774.
21. Liu, X. Q.; Li, C. C.; Zhang, D.; Xiao, Y. N. *Macromol Chem Phys* 2006, 207, 694.
22. Xiao, J.; Wan, X. H.; Zhang, D.; Zhang, H. L.; Zhou, Q. F.; Turner, S. R. *J Polym Sci Part A: Polym Chem* 2002, 40, 852.
23. Avrami, M. *J Chem Phys* 1939, 7, 1103.
24. Avrami, M. *J Chem Phys* 1940, 8, 212.
25. Mandelkern, M. *Methods of Experimental Physics, Part B*; Academic Press: New York, 1980; Vol. 16.
26. Jeziorny, A. *Polymer* 1978, 19, 1142.
27. Seong, H. K.; Seon, H. A.; Toshihiro, H. *Polymer* 2003, 44, 5625.
28. Ozawa, T. *Polymer* 1971, 12, 150.
29. Pitt, S.; Nujalee, D.; Phornphon, S.; Manit, N. *Thermochim Acta* 2003, 406, 207.
30. Liu, X. Q.; Li, C. C.; Zhang, D.; Xiao, Y. N. *J Polym Sci Part B: Polym Phys* 2006, 44, 900.
31. Khanna, Y. P. *Polym Eng Sci* 1990, 30, 1615.
32. Liu, H. Z.; Yang, G. S.; He, A. H.; Wu, M. Y. *J Appl Polym Sci* 2004, 94, 819.
33. Yasuniwa, M.; Satou, T. *J Polym Sci Part B: Polym Phys* 2002, 40, 2411.
34. Qiu, Z. B.; Komura, M.; Ikehara, T.; Nishi, T. *Polymer* 2003, 44, 7781.
35. Nattapol, A.; Pitt, S.; Manit, N. *Polym Test* 2004, 23, 817.